

Frascati Physics Series Vol. VVVVVV (xxxx), pp. 000-000
THE 2nd PANDA PHYSICS WORKSHOP – Frascati, March 18 - 19, 2004

HOW TO STUDY QUARK SPIN WITHOUT SPIN

Marco Radici

Istituto Nazionale di Fisica Nucleare - Sezione di Pavia - Pavia - Italy

ABSTRACT

I review the most important single- and double-spin asymmetries that allow for the extraction of transversity and other chiral-odd and/or T-odd parton densities, necessary to explore the partonic content and the spin structure of the nucleon. With particular reference to the proposed GSI-HESR facility, I report on some Monte-Carlo simulations of cross sections and spin asymmetries for (un)polarized Drell-Yan with protons and antiprotons at the proposed kinematics for this future facility.

1 Introduction

Recently, several experimental collaborations reported on nonvanishing single-spin asymmetries (SSA) in hard processes involving a target with a nonnegligible percentage of transverse polarization \mathbf{S}_T (1, 2). Historically, the first

discussion about transverse-spin effects in high-energy physics goes back to the late seventies, when an anomalous large transverse polarization of the Λ produced in pN annihilations was measured, surviving even at large values of transverse momentum p_T ³⁾. Such an observation requires a nonvanishing imaginary part in the off-diagonal part of the fragmentation matrix of quarks into Λ , which is forbidden in QCD at leading twist and appears as a $\mathcal{O}(1/p_T)$ effect ⁴⁾. A pioneering work soon appeared ⁵⁾ about the possibility of having leading-twist asymmetries in fully polarized Drell-Yan processes, but it was basically ignored for almost a decade upon the prejudice that transverse-spin effects have to be suppressed.

The above quoted recent observations warn us about two fundamental issues. First of all, even the leading-order (transverse) spin structure of the nucleon (and of hadrons, in general) is far from being fully understood. Secondly, SSA signal the appearance of effects that cannot be explained by perturbative QCD, because they are essentially related to a correlation between the polarization and the nonperturbative intrinsic transverse momentum of quarks, as well as to their orbital motion inside the parent hadron. Such features can co-exist in objects linked to processes flipping the quark helicity and/or describing residual interactions between the quark and the surrounding hadronic matter, such that the invariance upon time-reversal does not put any constraint. In common jargon, the first group is made of chiral-odd functions, since at leading twist chirality and helicity are identical ⁶⁾; QCD does preserve helicity, so these functions pertain the "soft" domain where the chiral symmetry of QCD is (spontaneously) broken. The most important one is a parton density related to the distribution of the transverse polarization of quarks in transversely polarized hadrons. It is a leading-twist parton distribution function (PDF), therefore necessary to complete the knowledge of the partonic spin structure of hadrons, but it escaped notice so far because of its chiral-odd nature, which prevents it from being extracted in most common processes like inclusive Deep-Inelastic Scattering (DIS) ⁶⁾. In Sec. 2, I will briefly review its main properties (for a more thorough review see ref. ⁷⁾).

The second group of functions is named, in jargon, T-odd: it does not mean a violation of the fundamental law of nature, it simply indicates that the above mentioned residual interactions prevent the time-reversal operation to put any constraint on such functions. Nevertheless, for several years a common

prejudice prevented people from recognizing the existence of such objects both as PDF and parton fragmentation functions (PFF), and led them to reject the possibility of asymmetries in processes like $pp^\dagger \rightarrow \pi X$ because of the violation of invariance under time-reversal transformations. The above mentioned recent observation of such an asymmetry clearly contradicts such prejudice. The most famous example of T-odd functions is the Collins function ⁸⁾, that I will recall in Sec. 3 together with other similar objects, the interference fragmentation functions (IFF) ^{9, 10)}.

The rich scenario depicted above, obtained by releasing some of the constraints introduced by standard perturbative QCD, lead to even more "exotic", but useful, conclusions. In fact, the existence of chiral-odd and/or T-odd PDF (PFF) allows for the description of the polarization state of quarks irrespectively of the polarization state of the parent hadron; it is then truly possible to perform spin physics without using polarized targets. In Sec. 4, I will recall how the combination of unpolarized and polarized Drell-Yan processes, particularly involving antiprotons, can help us in disentangling the unknown PDF and PFF occurring elsewhere, like in semi-inclusive DIS (SIDIS) or proton annihilation. In the last section, Sec. 5, I will explicitly show some Monte-Carlo simulations for such Drell-Yan processes in the kinematics of interest for the GSI-HESR future facility.

2 Transversity

At leading twist, three PDF are needed to describe the partonic spin structure of the nucleon. The easiest and most intuitive way to see it is to expand the PDF on the quark-nucleon helicity basis ⁹⁾,

$$\begin{aligned} \text{PDF}(x, Q^2) = & \frac{1}{2} q(x, Q^2) I \otimes I + \frac{1}{2} \Delta q(x, Q^2) \sigma_3 \otimes \sigma_3 \\ & + \frac{1}{2} \delta q(x, Q^2) [\sigma_+ \otimes \sigma_- + \sigma_- \otimes \sigma_+] . \end{aligned} \quad (1)$$

The functions $q, \Delta q$, are the momentum and helicity distributions, which are well known experimentally and have a clear probabilistic interpretation. The function δq is not diagonal in the helicity basis; it mixes different helicity (hence, chirality) states and, therefore, it is suppressed in one of the simplest measurable processes, the inclusive DIS (fig. 1). For this reason it escaped notice until recently. But it is a fundamental piece of information about the nucleon spin

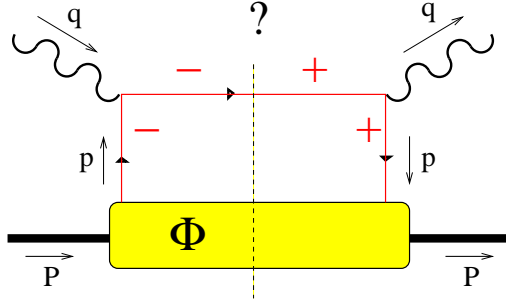


Figure 1: *The main contribution to inclusive DIS. Intermediate quark helicity states are also indicated.*

structure, with the same dignity as the other two PDF. In fact, by changing from the helicity to the transverse spin basis, the role of Δq and δq is interchanged; now, δq is diagonal and can be interpreted as the probability to find a quark with its spin polarized along the transverse spin of a polarized nucleon minus the probability to find it polarized oppositely ⁶⁾. In the following, I will switch to the more common notations of f_1, g_1 and h_1 for the three PDF discussed above: f will always indicate unpolarized partons, while by g, h , I mean their longitudinal and transverse polarization, respectively; finally, the index ₁ indicates that these PDF happen at leading twist. The situation is graphically summarized in fig. 2.

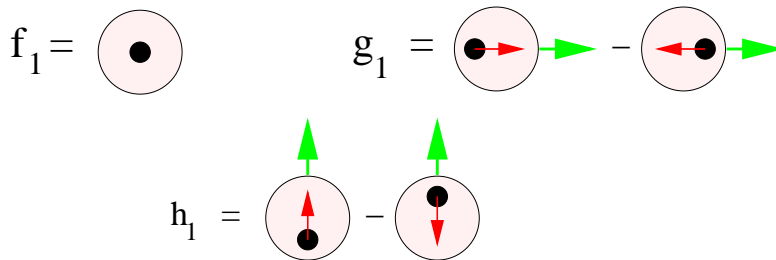


Figure 2: *The probabilistic interpretation of f_1, g_1 , and h_1 , respectively.*

Contrary to the other two PDF, the transversity h_1 does not have a counterpart in the Quark Parton Model (QPM) at the level of DIS structure function, because of its chiral-odd nature. Even if it depends on spin, it is not related to a partonic fraction of the nucleon spin, because the related twist-2 operator is not part of the full angular momentum tensor. The first moment of h_1^f , for a quark with flavor f in a nucleon state $|PS\rangle$ with momentum P and spin S , is called the tensor charge, i.e.

$$\begin{aligned} \langle PS|\bar{q}^f i\sigma^{0i}\gamma_5 q^f|PS\rangle \Big|_{Q^2} &= 2S^i \int dx \left[h_1^f(x, Q^2) - \bar{h}_1^f(x, Q^2) \right] \\ &= 2S^i \delta q^f(Q^2) \sim \frac{1}{(\log Q^2)^\gamma}, \end{aligned} \quad (2)$$

because it is related to the tensor operator $\sigma^{\mu\nu}\gamma_5$; it has a nonvanishing anomalous dimension γ and, therefore, from a renormalization scale Q^2 it evolves unavoidably to zero ⁶⁾. On the contrary, the nonsinglet axial charge $2S^i \Delta q^f(Q^2)$ is directly related to the nucleon axial charge g_A so that the corresponding distribution $g_1(x, Q^2)$ truly describes the quark helicity as a fraction of the nucleon's one. The other big difference can be read from eq. 2, namely the transversity for the antiquark enters with an opposite sign such that δq^f is odd under charge conjugation operations, contrary to Δq^f . This means that, under evolution, h_1 does not mix with charge-even structures like the $q\bar{q}$ pairs from the Dirac sea. If we now realize that δq^f cannot mix also with gluonic operators, which are both chiral- and charge-even in a spin $\frac{1}{2}$ hadron, we come to the conclusion that the transversity has very peculiar evolution properties: each moment does depend on the scale Q^2 , but the function evolves homogeneously with Q^2 like a pure nonsinglet structure function, completely decoupled from gluons and $q\bar{q}$ pairs ⁶⁾. It is probably the best place to explore the valence quark content of the nucleon and to test models based on the concept of constituent quark.

From eq. 1 it is evident that g_1 is associated to the operator σ_3 while h_1 to σ_1 (or σ_2 by a rotation in the spin space around \hat{z}). Since in the nonrelativistic framework spin and space operations (Euclidean boosts, etc..) commute, we easily get $g_1 = f_1$, as it is also graphically intuitive from fig. 2. Therefore, any deviation from this equality will tell us about the relativistic nature of quark motion in the nucleons, as much as the nonrelativistic prediction $g_A = \frac{5}{3}$ deviates from the experimental value of 1.255 ± 0.006 ¹¹⁾.

Finally, from the positivity of probability distributions we get

$$\begin{aligned} |g_1^f(x, Q^2)| &\leq f_1^f(x, Q^2) \\ |h_1^f(x, Q^2)| &\leq f_1^f(x, Q^2), \end{aligned} \quad (3)$$

while from the quark distribution matrix of eq. 1 in helicity basis being semi-positive definite, we get the so-called Soffer inequality ¹²⁾,

$$f_1^f(x, Q^2) + g_1^f(x, Q^2) \geq 2|h_1^f(x, Q^2)|, \quad (4)$$

which holds up to next-to-leading order in QCD radiative corrections ^{13, 14)}.

3 Transversity from semi-inclusive processes

Since the transversity h_1 is a chiral-odd PDF happening at leading twist, we need to find a leading-twist chiral-odd partner in order to extract it from the cross section. There are two possibilities: a polarized Drell-Yan process where h_1 happens in combination with the transversity \bar{h}_1 for an antiquark, or a semi-inclusive process, where h_1 is combined with a chiral-odd PFF. Despite the fact that the extraction of h_1 from Drell-Yan was suggested as first in the literature long time ago ⁵⁾, we will postpone it to the next sec. 4. Here in the following, we will discuss SIDIS or annihilation processes leading to the Collins effect and other interesting phenomena.

3.1 One-hadron semi-inclusive processes

Since we are looking for a semi-inclusive process where transverse polarization is involved at the partonic level, we are naturally led to select a final state with a transversely polarized hadron. The most natural choice is the hyperon Λ , whose polarization is easily deduced from the angular distribution of its decay products. For the electroproduction of transversely polarized Λ on a transversely polarized proton, $ep^\uparrow \rightarrow e'\Lambda^\uparrow X$, the leading contribution comes from the well known handbag diagram (see fig. 3); h_1 can then be extracted by the double-spin asymmetry (DSA, or depolarization or spin transfer coefficient, as differently reported in the literature) ¹⁵⁾

$$D_{NN} = \frac{d\sigma(p^\uparrow\Lambda^\uparrow) - d\sigma(p^\downarrow\Lambda^\uparrow)}{d\sigma(p^\uparrow\Lambda^\uparrow) + d\sigma(p^\downarrow\Lambda^\uparrow)} \propto |\mathbf{S}_T||\mathbf{S}_{\Lambda_T}| \frac{\sum_f e_f^2 h_1^f(x) H_1^f(z)}{\sum_f e_f^2 f_1^f(x) D_1^f(z)}, \quad (5)$$

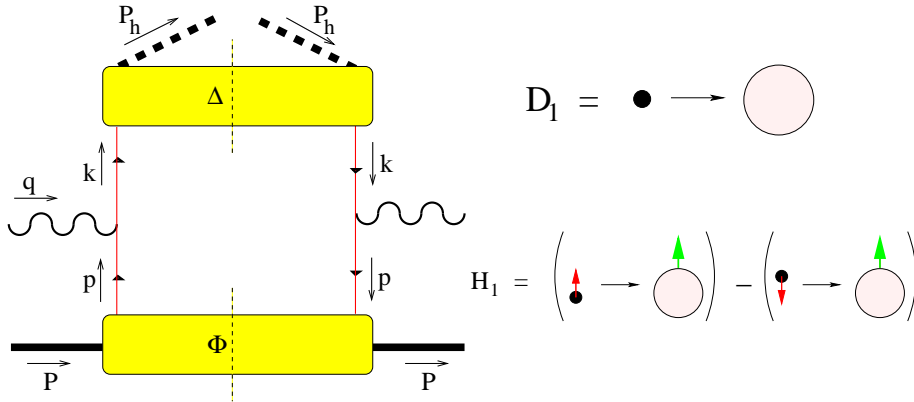


Figure 3: *The handbag diagram, the leading contribution to SIDIS, and the probabilistic interpretation of D_1 and H_1 .*

where D_1 is the PFF of an unpolarized quark into the unpolarized Λ and H_1 is its partner for the transversely polarized case (see fig. 3; the notations follow the same convention as for the PDF, but with upper case letters and with the exception of D_1 , in order not to be confused with the DIS structure function F_1). On the experimental side, the DSA has been measured also for the reaction $pp^\uparrow \rightarrow \Lambda^\uparrow X$ ¹⁶⁾, which has the same partonic content as eq. 5 but for an additional \bar{f}_1 for the annihilating unpolarized antiquark. On the theoretical side, the problem is related to the identification of the spin transfer mechanism: while it is somewhat clear how to reproduce the Λ properties from the uds valence picture using $SU_f(3)$, it is not at all clear how the transverse polarization of the fragmenting quark is transferred to the transversely polarized Λ . Several models are available in the literature (for example, see ref. ¹⁷⁾); the use of polarized proton and antiproton beams at GSI would help in selecting them, also because the PDF of an antiquark is not suppressed in an antiproton.

The second option is to transfer the transverse polarization of a fragmenting quark to an unpolarized hadron with an explicit dependence on its transverse momentum $\mathbf{P}_{h\perp}$. The leading contribution is again given by the handbag diagram of fig. 3, but the azimuthal asymmetry is now determined by the T-odd mixed product $\sin\phi_c \propto \mathbf{k} \times \mathbf{P}_{h\perp} \cdot \mathbf{S}_T$ ⁸⁾, as represented in fig. 4, where ϕ_c is the so-called Collins angle. An explicit dependence of the

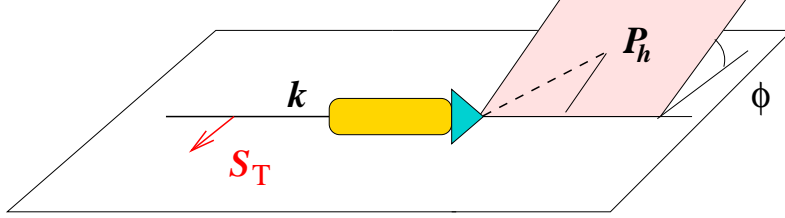


Figure 4: *The Collins mechanism.*

$$\mathbf{H}_1^\perp = \left(\begin{array}{c} \uparrow \\ \bullet \end{array} \rightarrow \text{circle} \right) - \left(\begin{array}{c} \bullet \\ \downarrow \end{array} \rightarrow \text{circle} \right)$$

Figure 5: *The Collins function.*

cross section on $\mathbf{P}_{h\perp}$ implies a sensitivity to the transverse momenta of the partons involved in the hard vertex. For the handbag diagram of fig. 3, the leading-twist decomposition of the quark-quark correlators Φ and Δ depending explicitly on the quark transverse momenta \mathbf{p}_T and \mathbf{k}_T , respectively, shows a very rich structure¹⁸⁾, where $h_1(x, \mathbf{p}_T)$ appears convoluted with the Collins function $H_1^\perp(z, \mathbf{k}_T)$, a chiral-odd and T-odd PFF whose probabilistic interpretation is depicted in fig. 5 (the "⊥" notation indicates that the Collins function appears weighted by the transverse momentum \mathbf{k}_T).

Such a SSA has been observed at SMC for the $pp^\uparrow \rightarrow \pi X$ reaction, but with a very low resolution in the final state¹⁾. The Collins effect has been observed also for the process $ep^\uparrow \rightarrow e'\pi X$ ²⁾, but using a target polarized along the beam direction with a consequent small fraction of transverse polarization with respect to the momentum transfer q . For this setup, both the cross section for longitudinally and transversely polarized targets do contribute at leading and subleading twist, since $|\mathbf{S}_T|$ is suppressed by a factor $1/Q$ with respect to the helicity λ . Several contributions mix up in the SSA and it is not easy

to select the combination corresponding to the Collins effect (for a detailed discussion, see for example ref. 19)).

Only recently, data were taken at HERMES with a pure transversely polarized target. In this case, the six-fold differential cross section reads 20)

$$\begin{aligned} \frac{d^6\sigma_{OT}}{dx dy dz d\phi_s d\mathbf{P}_{h\perp}} &\propto |\mathbf{S}_T| \left\{ \sin(\phi_h + \phi_s) \mathcal{F} \left[\frac{\mathbf{k}_T \cdot \hat{h}}{M_h} x h_1(x, \mathbf{p}_T^2) H_1^\perp(z, \mathbf{k}_T^2) \right] \right. \\ &+ \sin(\phi_h - \phi_s) \mathcal{F} \left[\frac{\mathbf{p}_T \cdot \hat{h}}{M} x f_{1T}^\perp(x, \mathbf{p}_T^2) D_1^\perp(z, \mathbf{k}_T^2) \right] \\ &\left. + \sin(3\phi_h - \phi_s) \mathcal{F} [a(\mathbf{p}_T, \mathbf{k}_T) h_{1T}^\perp(x, \mathbf{p}_T^2) H_1^\perp(z, \mathbf{k}_T^2)] \right\} , \end{aligned} \quad (6)$$

where M, M_h are the proton and pion masses, respectively, and the convolution is defined as

$$\mathcal{F}[\dots] \equiv \int d\mathbf{p}_T d\mathbf{k}_T \delta(\mathbf{p}_T + \mathbf{q}_T - \mathbf{k}_T) \dots , \quad (7)$$

with \mathbf{q}_T the transverse component of the momentum transfer in the hard vertex. If the lab plane is defined by the directions of the beam and of the target polarization vector, then the azimuthal angles ϕ_s, ϕ_h in eq. 6 represent the orientation of the lab plane and final hadronic plane (formed by $\mathbf{P}_{h\perp}$ and \mathbf{q}) with respect to the scattering plane, respectively. The contribution corresponding to the Collins effect ($\sin\phi_c \equiv \sin(\phi_s + \phi_h)$) can be extracted by the following SSA 20)

$$\begin{aligned} \left\langle \frac{\mathbf{P}_{h\perp}}{M_h} \sin\phi_c \right\rangle &\equiv \frac{\int d\phi_s d\mathbf{P}_{h\perp} \sin\phi_c [d\sigma(p^\uparrow) - d\sigma(p^\downarrow)]}{\int d\phi_s d\mathbf{P}_{h\perp} [d\sigma(p^\uparrow) + d\sigma(p^\downarrow)]} \\ &\propto |\mathbf{S}_T| \frac{\sum_f e_f^2 x h_1^f(x) H_1^{\perp f(1)}(z)}{\sum_f e_f^2 f_1^f(x) D_1^f(z)} , \end{aligned} \quad (8)$$

where $H_1^{\perp f(1)}(z) = \int d\mathbf{k}_T \frac{\mathbf{k}_T^2}{2M_h} H_1^\perp(z, \mathbf{k}_T^2)$ is the first moment of the Collins function (the simple $\langle \sin\phi_c \rangle$ does not break the convolution, unless some assumption on the \mathbf{p}_T and \mathbf{k}_T dependence of the functions is made). Eq. 8 implies that, when calculating the radiative corrections in order to determine its QCD evolution, the explicit $\mathbf{P}_{h\perp}$ dependence breaks the collinear factorization and forces to resum all the contributions of real and virtual soft gluons into the so-called Sudakov form factors, which can largely dilute the SSA 21). The same

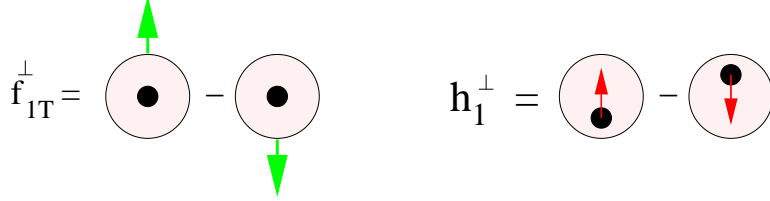


Figure 6: *The Sivers and the "Boer" functions on the left and the right, respectively.*

problem appears when trying to extract information on the Collins function via the corresponding $e^+e^- \rightarrow \pi^+\pi^-X$ reaction, as it is somewhat confirmed by the analysis of the DELPHI data collection where an asymmetry of at most 6% is observed²²⁾ (but with large uncertainties).

The second term in eq. 6 represents the so-called Sivers effect²³⁾, because it is driven by the chiral-even T-odd Sivers function f_{1T}^\perp that describes how the distribution of unpolarized quarks is affected by the transverse polarization of the parent hadron (see fig. 6), from which the notation " $_T$ " originates. As it is evident from its azimuthal dependence, this effect can be disentangled by the Collins one only if the target polarization vector sticks out of the scattering plane, i.e. $\phi_s \neq 0$. The situation is potentially more confused in the annihilation process $pp^\uparrow \rightarrow \pi X$, where the Collins and Sivers effects do not exhaust all the possibilities. In fact, at leading twist one more combination generates a similar azimuthal asymmetry, namely the SSA²⁴⁾

$$\frac{d\sigma(p^\uparrow) - d\sigma(p^\downarrow)}{d\sigma(p^\uparrow) + d\sigma(p^\downarrow)} \propto \frac{\sum_f h_1^{\perp f}(x_1) \bar{h}_1^f(x_2) D_1^f(z)}{\sum_f f_1^f(x_1) \bar{f}_1^f(x_2) D_1^f(z)}, \quad (9)$$

where h_1^\perp is a twist-2 chiral-odd T-odd PDF describing the influence of the quark transverse polarization on its momentum distribution inside an unpolarized parent hadron (see fig. 6). Moreover, even if the involved PDF appear at leading twist, the required explicit dependence of the elementary cross section on transverse momenta of the partons introduces a suppression factor, raising the relative importance of subleading-twist effects like the Qiu-Stermann one²⁵⁾.

3.2 Color-gauge invariance and T-odd parton densities

In the previous section, we encountered several examples of T-odd PDF and PFF that appear as soon as we allow them to depend explicitly on the parton transverse momentum; in fact, integration upon the latter washes all these effects away.

We already mentioned that the jargon "T-odd" indicates no constraints on the considered function from the invariance under time-reversal transformation. For the Collins function, this can be simply interpreted by advocating residual Final State Interactions (FSI) occurring between the detected hadron and the residual jet. As soon as we reduce the hadron wave function to a plane wave, the time-reversal invariance forbids the Collins effect and makes H_1^\perp to vanish; but in reality there are FSI between this hadron and the jet on a time scale much longer than the hard vertex, hence the *in* and *out* states cannot be interchanged and the invariance under time-reversal does not put any constraint: T-odd structures are allowed and we observe the Collins effect.

But how to interpret the T-odd PDF f_{1T}^\perp and h_1^\perp ? If for the $pp^\uparrow \rightarrow \pi X$ process we can think about a sort of Initial State Interaction (ISI) occurring before the hard annihilation (26, 27, 28), we cannot recycle the same idea in the SIDIS process $ep^\uparrow \rightarrow e'\pi X$. However, there is another "technical" consideration that leads to T-odd structures. The PDF can be obtained as suitable Dirac projections of the quark-quark correlator

$$\Phi(x, S) = \int \frac{d\zeta^-}{2\pi} e^{ixP^+\zeta^-} \langle P, S | \bar{\psi}(0) U_{[0, \zeta^-]} \psi(\zeta) | P, S \rangle \Bigg|_{\zeta^+ = \vec{\zeta}_T = 0}, \quad (10)$$

which is made color-gauge invariant by the introduction of the so-called gauge link operator

$$U_{[0, \zeta]} = \mathcal{P} e^{-ig \int_0^\zeta dw \cdot A(w)}, \quad (11)$$

linking the two different space-time points $0, \zeta$, by all the possible ordered paths ($\mathcal{P}[\dots]$) followed by the gluon field A , which couples to the quark field ψ by the constant g . Since the interaction in eq. 10 runs along the suppressed "-" direction, the longitudinal A^+ component of the gluon field appears at any power in the expansion of the exponential; therefore, a possible representation of the gauge link operator is depicted in the diagram of fig. 7. Hence, a sort of residual FSI occurs between the parton and the residual hadron, opening the

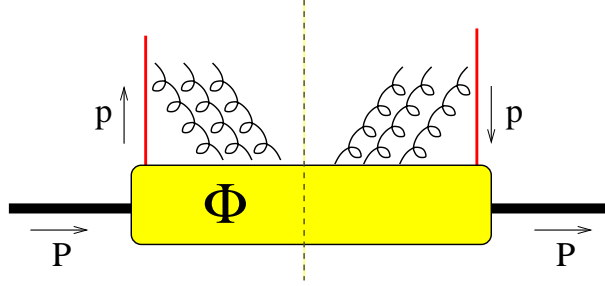


Figure 7: A possible representation of the color-gauge invariant quark-quark correlator.

possibility for T-odd structures²⁹). When also the \mathbf{p}_T dependence is explicitly kept in eq. 10, the path required to connect at leading twist the points $[0, \zeta]$ is more complicated and involves also the \mathbf{A}_T component of the gluon field²⁹), but the bulk of the message is unchanged.

3.3 Interference Fragmentation Functions

In sec. 3.1, we stressed the difficulties arising when the cross section must be kept differential also on the transverse momentum of the detected hadron, namely the appearance of other effects, contributing to the same asymmetry as the Collins effect, or the breaking of collinear factorization when computing radiative corrections beyond leading order. For these reasons, it is desirable to find a mechanism that leads to T-odd structures surviving the integration upon transverse momenta. This requirement is fulfilled by the semi-inclusive process where two leading hadrons are detected in the same jet. The asymmetry happens, then, in the azimuthal angle $\sin \phi \propto \mathbf{P}_1 \times \mathbf{P}_2 \cdot \mathbf{S}_T = \mathbf{P}_h \times \mathbf{R} \cdot \mathbf{S}_T$, where $P_h = P_1 + P_2$ and $R = (P_1 - P_2)/2$ are the total and relative momentum of the final pair (see fig. 8)³⁰). If the two hadrons are unpolarized, four PFF appear by projecting the leading-twist contributions of the proper quark-quark correlator Δ ¹⁰): the probability of an unpolarized quark to fragment into two unpolarized hadrons, D_1 ; the probability of a quark with positive helicity to fragment into two hadrons minus the same probability but with negative helicity, G_1^\perp ; and, finally, the same probability difference for a transversely polarized quark, occurring in the combination $\mathbf{k}_T H_1^\perp + \mathbf{R}_T H_1^\triangleleft$ (see fig. 9). More

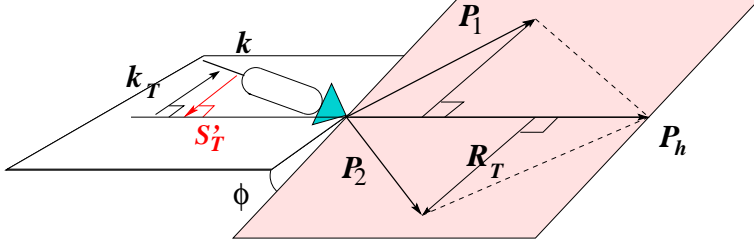


Figure 8: *The Collins-Ladinski (CL) mechanism.*

complicated structures appear at subleading twist, involving also the quark-gluon-quark correlator³¹⁾. As for the projection by the tensor operator, H_1^\perp is the analogue of the Collins function, while H_1^\triangleleft is related to a truly new effect. In fact, the transverse polarization of the fragmenting quark is transformed into the orbital relative motion of the hadron pair via the vector \mathbf{R}_T : the azimuthal distribution of the two hadrons in the detector depends on the transverse polarization of the quark. All these functions, which are T-odd but for D_1 , are related to the residual interactions between the two hadrons inside the jet; therefore, they are usually referred to as Interference Fragmentation Functions (IFF)^{9, 10)}. Moreover, H_1^\perp and H_1^\triangleleft are chiral-odd. They have a rather complicated structure. Their functional dependence can conveniently be chosen as the light-cone fraction of the quark momentum carried by the hadron pair, $z = P_h^-/k^- = (P_1^- + P_2^-)/k^- = z\xi + z(1-\xi)$, the subfraction in which this momentum is further shared inside the pair, ξ , and the "geometry" of the pair in the momentum space: the "opening" of the pair momenta, \mathbf{R}_T^2 , the relative position of the jet axis and the hadron pair axis, \mathbf{k}_T^2 , and the relative position of the hadron pair plane and the plane formed by the jet axis and the hadron pair axis, $\mathbf{k}_T \cdot \mathbf{R}_T$ ¹⁰⁾ (see fig. 8).

After integrating on $\mathbf{P}_{h\perp}$, the leading-twist nine-fold differential cross section for the $ep^\uparrow \rightarrow e'(\pi\pi)X$ process becomes³²⁾

$$\frac{d\sigma_{OT}}{dx dy dz d\xi dM_h^2 d\phi_S d\phi_R} \propto \frac{|\mathbf{S}_T||\mathbf{R}_T|}{M_h} \sin(\phi_S + \phi_R) h_1(x) H_1^\triangleleft(z, \xi, M_h^2), \quad (12)$$

where the role of ϕ_h in eq. 6 is here taken over by ϕ_R , and the dependence on M_h^2 is due to the relation $\mathbf{R}_T^2 = \xi(1-\xi)M_h^2 - (1-\xi)M_1^2 - \xi M_2^2$. The important fact

$$\begin{aligned}
D_1 &= \bullet \longrightarrow \begin{array}{c} \text{small circle} \\ \text{large circle} \end{array} & G_1^\perp &= \left(\begin{array}{c} \bullet \xrightarrow{\text{red arrow}} \\ \text{large circle} \end{array} \right) - \left(\begin{array}{c} \bullet \xleftarrow{\text{red arrow}} \\ \text{large circle} \end{array} \right) \\
H_1^\perp, H_1^{\not\leftarrow} &= \left(\begin{array}{c} \bullet \xrightarrow{\text{red arrow up}} \\ \text{large circle} \end{array} \right) - \left(\begin{array}{c} \bullet \xrightarrow{\text{red arrow down}} \\ \text{large circle} \end{array} \right)
\end{aligned}$$

Figure 9: *The Interference Fragmentation Functions at leading twist.*

here is that, even after integration on the transverse momenta of all particles, still a T-odd PFF survives, $H_1^{\not\leftarrow}$, because there is another transverse momentum, \mathbf{R}_T , available to generate an azimuthal asymmetry. Luckily, $H_1^{\not\leftarrow}$ is also chiral-odd and, therefore, it represents a perfect partner to isolate transversity. In fact, the corresponding SSA is ³²⁾

$$\begin{aligned}
A_{OT}^{\sin\phi} &= \frac{\int d\phi_s d\phi_R d\xi \sin(\phi_s + \phi_R) [d\sigma(p^\uparrow) - d\sigma(p^\downarrow)]}{\int d\phi_s d\phi_R d\xi [d\sigma(p^\uparrow) + d\sigma(p^\downarrow)]} \\
&\propto |\mathbf{S}_T| \frac{\sum_f e_f^2 h_1^f(x) \int d\xi d\phi_R \frac{|\mathbf{R}_T|}{2M_h} H_{1(R)}^{\not\leftarrow f}(z, \xi, M_h^2)}{\sum_f e_f^2 f_1^f(x) D_1^f(z, M_h^2)} \\
&\equiv |\mathbf{S}_T| \frac{\sum_f e_f^2 h_1^f(x) H_{1(R)}^{\not\leftarrow f}(z, M_h^2)}{\sum_f e_f^2 f_1^f(x) D_1^f(z, M_h^2)}, \tag{13}
\end{aligned}$$

where the specific moment $H_{1(R)}^{\not\leftarrow f}$ is involved. The very same moment appears when considering the corresponding $e^+e^- \rightarrow (\pi\pi)_{jet1}(\pi\pi)_{jet2}X$ process at leading twist and looking for an azimuthal asymmetry in the position of the pion pair planes with respect to the lab frame ³³⁾. Even if a factorization theorem is not yet proven for IFF, the universality holds, at least at leading twist, allowing to extract informations on the unknown function $H_1^{\not\leftarrow}$. Moreover, because of the disappearance of any transverse momenta of involved particles all the difficulties arising for the Collins effect are here overcome: collinear factorization holds, avoiding any dilution of SSA by Sudakov form factors; the analogue of

the Sivers effect is here absent, keeping formulae simpler; in the corresponding annihilation $pp^\uparrow \rightarrow (\pi\pi)X$ the elementary cross section does not depend on transverse parton momenta, so that the result is truly a leading-twist one ³⁴).

Another advantage of IFF is the possibility of studying in some detail the FSI responsible for the T-odd structures. For example, if the two unpolarized hadrons are two pions, in their center-of-mass frame the IFF can be expanded in relative partial waves retaining the main contributions, which for two pions are the s and p waves ³⁵). Therefore, since FSI arise from the interference of different channels with different phases, two possible sources of interference appear: the $s - p$ ⁹) and the $p - p$ ones. Both these components of H_1^\triangleleft act in the SSA of eq. 13 and can be disentangled by a suitable selection of the integration phase space ³⁵). In particular, the latter is formally and closely related to the fragmentation of spin-1 objects, like the ρ polarized fragmentation functions ³⁶).

When considering two leading unpolarized hadrons inside the jet of the current fragmentation region, another interesting azimuthal asymmetry can be built for the $e^+e^- \rightarrow (\pi\pi)_{jet1}(\pi\pi)_{jet2}X$ process, which involves the helicity IFF G_1^\perp ³³):

$$\begin{aligned}
\langle \cos 2(\phi_R - \bar{\phi}_R) \rangle &= \frac{\int d\xi d\phi_R d\bar{\xi} d\bar{\phi}_R d\mathbf{q}_T \cos 2(\phi_R - \bar{\phi}_R) d\sigma}{\int d\xi d\phi_R d\bar{\xi} d\bar{\phi}_R d\mathbf{q}_T d\sigma} \\
&\propto \frac{\sum_f e_f^2 \int d\xi d\phi_R d\mathbf{k}_T \mathbf{k}_T \cdot \mathbf{R}_T G_1^{\perp f}(z, \xi, \mathbf{k}_T^2, \mathbf{R}_T^2, \mathbf{k}_T \cdot \mathbf{R}_T)}{\sum_f e_f^2 \int d\xi d\phi_R d\mathbf{k}_T D_1^f(z, \xi, \mathbf{k}_T^2, \mathbf{R}_T^2, \mathbf{k}_T \cdot \mathbf{R}_T)} \\
&\quad \times \frac{\int d\bar{\xi} d\bar{\phi}_R d\bar{\mathbf{k}}_T \bar{\mathbf{k}}_T \cdot \bar{\mathbf{R}}_T \bar{G}_1^{\perp f}(\bar{z}, \bar{\xi}, \bar{\mathbf{k}}_T^2, \bar{\mathbf{R}}_T^2, \bar{\mathbf{k}}_T \cdot \bar{\mathbf{R}}_T)}{\int d\bar{\xi} d\bar{\phi}_R d\bar{\mathbf{k}}_T \bar{D}_1^f(\bar{z}, \bar{\xi}, \bar{\mathbf{k}}_T^2, \bar{\mathbf{R}}_T^2, \bar{\mathbf{k}}_T \cdot \bar{\mathbf{R}}_T)} \\
&\equiv \frac{\sum_f e_f^2 G_{1\otimes}^{\perp f}(z, M_h^2) \bar{G}_{1\otimes}^{\perp f}(\bar{z}, \bar{M}_h^2)}{\sum_f e_f^2 D_1^f(z, M_h^2) \bar{D}_1^f(\bar{z}, \bar{M}_h^2)}. \tag{14}
\end{aligned}$$

When integrating directly on \mathbf{k}_T , G_1^\perp vanishes because of parity invariance. However, the asymmetry in the azimuthal relative position of the planes of the two pion pairs involves the specific nonvanishing "moment" $G_{1\otimes}^\perp$, which allows for a relation between the longitudinal polarization of the fragmenting quark and the transverse relative motion of the hadron pair. This is a unique feature of IFF describing fragmentation into two unpolarized hadrons. The helicity analyzer G_1^\perp occurs weighted by the $(\mathbf{k}_T \times \mathbf{R}_T)$ factor in the leading-twist

projection; therefore, it is the closest analogue to the definition of longitudinal jet handedness³⁷⁾. It could be extracted from the cross section of the $e\bar{p} \rightarrow e'(\pi\pi)X$ process, where it appears at leading twist convoluted with the known helicity distribution g_1 . Assuming universality, it could be plugged inside eq. 14: a nonvanishing azimuthal asymmetry could then be the signal that a violation is taking place in the CP symmetry of the two back-to-back jets, maybe due to the effect of the nonperturbative vacuum of QCD³⁸⁾.

4 Transversity from Drell-Yan processes

As already anticipated in sec. 3, the polarized Drell-Yan process $p^\uparrow p^\uparrow \rightarrow l^+ l^- X$ was the first suggested in order to extract the transversity at leading order⁵⁾. In the so-called Collins-Soper frame, the \hat{z} axis is obtained by the "average" direction of the two annihilating hadron momenta, which lie in the hadronic plane rotated around \hat{z} by an azimuthal angle ϕ with respect to the lepton plane where the two leptons are emitted back-to-back at an angle θ with respect to \hat{z} (see fig. 10).

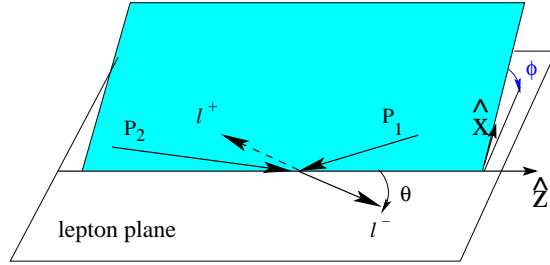


Figure 10: *The Collins-Soper frame for Drell-Yan processes.*

If the dominant contribution comes from the diagram depicted in fig. 11, then the following DSA,

$$\begin{aligned}
 A_{TT} &= \langle \cos(\phi_{s_1} + \phi_{s_2}) \rangle = \frac{\int d\mathbf{q}_T \cos(\phi_{s_1} + \phi_{s_2}) [d\sigma(p^\uparrow p^\uparrow) - d\sigma(p^\uparrow p^\downarrow)]}{\int d\mathbf{q}_T [d\sigma(p^\uparrow p^\uparrow) + d\sigma(p^\uparrow p^\downarrow)]} \\
 &= |\mathbf{S}_{T_1}| |\mathbf{S}_{T_2}| \frac{\sin^2 \theta \cos 2\phi}{1 + \cos^2 \theta} \frac{\sum_f e_f^2 h_1^f(x_1) \bar{h}_1^f(x_2)}{\sum_f e_f^2 f_1^f(x_1) \bar{f}_1^f(x_2)}, \quad (15)
 \end{aligned}$$

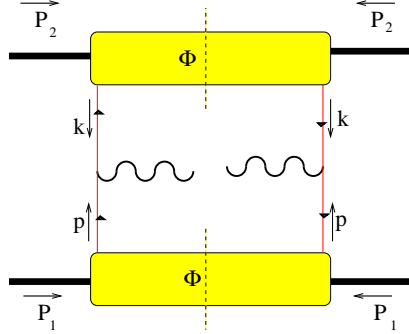


Figure 11: *The leading contribution to the Drell-Yan process.*

shows a factorized combination of transversities for the annihilating quark and antiquark at leading twist. The angles ϕ_{s_1}, ϕ_{s_2} , define the azimuthal position of the transverse polarization vectors of the two annihilating hadrons with respect to the lepton plane, while $x_{1/2} = Q^2/(2P_{1/2} \cdot q)$ and \mathbf{q}_T lies in the (\hat{x}, \hat{z}) plane of fig. 10. Unfortunately, in a NLO simulation A_{TT} turns out to be suppressed by the Soffer inequality and QCD evolution^{39, 40)}, and, moreover, it involves the transversity of an antiquark in a transversely polarized proton. The latter difficulty could be overcome at future GSI-HESR with polarized antiproton beams, where the asymmetry would involve transversities of valence partons anyway^{41, 42)}.

Also the single polarized and unpolarized Drell-Yan cross sections show interesting combinations at leading twist. For the $pp^\uparrow \rightarrow l^+l^-X$ process, the leading-twist cross section displays, among others, the following contributions²⁴⁾:

$$\begin{aligned} \frac{d\sigma}{dx_1 dx_2 d\Omega d\mathbf{q}_T} \propto |\mathbf{S}_{T_1}| \sum_f \left\{ \sin(\phi - \phi_{s_1}) \mathcal{F} \left[\hat{\mathbf{h}} \cdot \mathbf{p}_{T_1} f_{1T}^{\perp f}(x_1, \mathbf{p}_{T_1}) \bar{f}_1^f(x_2, \mathbf{p}_{T_2}) \right] \right. \\ \left. + \dots \sin(\phi + \phi_{s_1}) \mathcal{F} \left[\hat{\mathbf{h}} \cdot \mathbf{p}_{T_2} h_1^f(x_1, \mathbf{p}_{T_1}) \bar{h}_1^{\perp f}(x_2, \mathbf{p}_{T_2}) \dots \right] \right\}. \end{aligned} \quad (16)$$

The first term can be isolated by an azimuthal asymmetry similar to the one of the Sivers effect, in order to extract f_{1T}^\perp and compare it with the result of semi-inclusive processes (eq. 6): the different behaviour of the gauge link

operator in SIDIS and Drell-Yan processes leads to the interesting conjecture that a possible change of sign could take place, posing a question about the assumed universality of T-odd PDF (27, 29) (see also ref. (43)).

The second term in eq. 16 contains the transversity and can be isolated by an asymmetry similar to the Collins effect. However, h_1 appears convoluted with a second unknown function, h_1^\perp , which also contributes to the SSA for the $pp^\uparrow \rightarrow \pi X$ process. Interestingly, this function contributes also to the unpolarized Drell-Yan cross section at leading twist (24), i.e.

$$\frac{d\sigma}{dx_1 dx_2 d\Omega d\mathbf{q}_T} \propto \sum_f \left\{ \mathcal{F} \left[f_1^f \bar{f}_1^f \right] \dots \right. \\ \left. + \cos 2\phi \mathcal{F} \left[A(\mathbf{p}_{T_1}, \mathbf{p}_{T_2}) h_1^{\perp f}(x_1, \mathbf{p}_{T_1}) \bar{h}_1^{\perp f}(x_2, \mathbf{p}_{T_2}) \right] \dots \right\}, \quad (17)$$

where $A(\mathbf{p}_{T_1}, \mathbf{p}_{T_2})$ is some function of the transverse momenta of the annihilating partons. The crucial remark is that h_1^\perp can naturally explain the observed sizeable azimuthal asymmetry in unpolarized Drell-Yan cross sections. The most general parametrization of such cross sections at leading order looks like

$$\frac{1}{\sigma} \frac{d\sigma}{d\Omega} \propto 1 + \lambda \cos^2 \theta + \mu \sin^2 \theta \cos \phi + \frac{\nu}{2} \sin^2 \theta \cos 2\phi + o(\alpha_s), \quad (18)$$

where the data suggest $\lambda \sim 1$ and $\mu \ll \nu \sim 30\%$ (44), while the perturbative QCD gives $\lambda \sim 1, \mu \sim \nu \sim 0$. Neither higher twists, nor factorization-breaking terms of NLO contributions are able to justify such a big azimuthal asymmetry (45), while eq. 17 easily accounts for it because it contains a leading twist term $\sim \cos 2\phi$ and no contributions $\sim \cos \phi$. A simple explanation for this feature is the fact that, owing to its probabilistic interpretation (see fig. 6), each h_1^\perp carries one unit of quark orbital angular momentum L_z , introducing then a cosinusoidal dependence on twice the azimuthal angle ϕ .

In conclusion, the unpolarized Drell-Yan process allows for the extraction of a chiral-odd T-odd PDF, h_1^\perp , that can help in disentangling the transversity h_1 in the corresponding single-polarized Drell-Yan process and, in turn, to compare it with the one that can be extracted in SIDIS or annihilation processes. Even unpolarized observables can contribute to the study of spin structure of the nucleon. If beams of protons and antiprotons are used, as it will be at

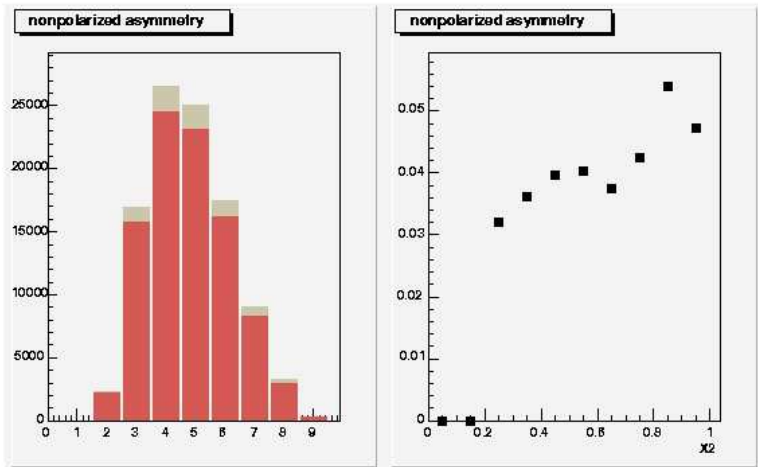


Figure 12: *Left panel: cross section for unpolarized Drell-Yan with antiproton beams in the kinematics of the ASSIA proposal; different histogram colors for different signs in the $\cos 2\phi$ azimuthal term. Right panel: the corresponding azimuthal asymmetry.*

GSI-HESR, the Drell-Yan azimuthal asymmetries will not be suppressed by nonvalence-like contributions.

5 Monte-Carlo simulations

In this section, some Monte-Carlo simulations are presented for the unpolarized and single-polarized Drell-Yan azimuthal asymmetries, involving proton and antiproton beams with the kinematical conditions discussed in the ASSIA proposal ⁴⁶). Very briefly, the considered process is $\bar{p}p^{(\uparrow)} \rightarrow \mu^+\mu^-X$ with an antiproton beam of $E_{\bar{p}} = 40$ GeV. The proton target is obtained by a NH_3 target with a dilution factor of $\frac{1}{4}$. When the target is polarized, a further 85% reduction is applied. The center-of-mass energy is $s \sim 2M_p E_{\bar{p}} \sim (9\text{GeV})^2$ and $\tau = x_1 x_2 = Q^2/s \leq 1$ for the invariant mass $Q \leq 9$ GeV. Finally, we have $-0.7 \leq x_F = x_1 - x_2 \leq 0.7$ for the invariant fraction of total longitudinal momentum with respect to the maximum available longitudinal momentum for the system of annihilating partons.

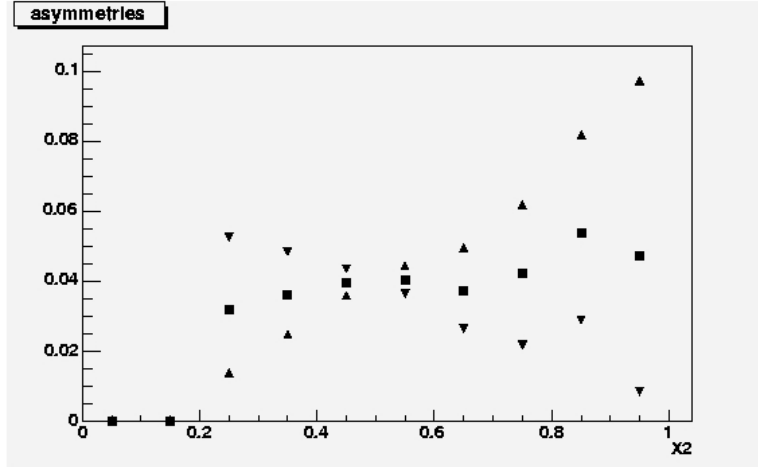


Figure 13: *The SSA for polarized Drell-Yan with antiproton beams in the kinematics of the ASSIA proposal. Upward triangles, squares, and downward triangles for different choices of the x_2 dependence (see text).*

The simulation consists of 480.000 events distributed according to the cross section

$$\frac{1}{\sigma} \frac{d\sigma}{d\Omega dx_1 dx_2 d\phi_{s_2}} = 1 + \cos^2 \theta + \frac{\nu(x_1, x_2, p_T)}{2} \sin^2 \theta \cos 2\phi + |\mathbf{S}_{T_2}| \sin^2 \theta \sin(\phi + \phi_{s_2}) A(x_1, x_2, p_T), \quad (19)$$

all the variables are represented in fig. 10 and p_T is the transverse momentum of the lepton pair. The latter is cut below 1 GeV/ c as well as the invariant mass of the muon pair, namely $M_{\mu\mu} > 4$ GeV.

In fig. 12, the left panel shows the cross section of eq. 19 for $|\mathbf{S}_{T_2}| = 0$ and binned in x_2 with positive and negative $\cos 2\phi$. The corresponding azimuthal asymmetry is shown in the right panel, which is proportional to $\nu(x_1, x_2, p_T)$ and is parametrized according to ref. 47). The obtained asymmetry around 5% seems measurable.

Next, in fig. 13 the same simulation in the same conditions is applied to the cross section of eq. 19 with $|\mathbf{S}_{T_2}| \neq 0$ and with different factorized behaviours for $A(x_1, x_2, p_T)$: upward triangles for $2(1 - x_2) A(x_1, p_T)$, squares

for $1 \cdot A(x_1, p_T)$, downward triangles for $2x_2 A(x_1, p_T)$. The function $A(x_1, p_T)$ is cancelled in the ratio of cross sections defining the azimuthal asymmetry; therefore, it needs not to be specified. The x_2 dependences represent three different "wild guesses" for the factorized ratio $h_1(x_2)/f_1(x_2)$ that appears in the asymmetry at leading twist. Despite the adopted crude approximations, the azimuthal asymmetry is sensitive enough to distinguish between these three choices, giving at the same time an average measurable result of around 5%.

In conclusion, Monte-Carlo simulations running antiproton beams on (polarized) proton targets at the kinematics of the ASSIA proposal at the GSI-HESR facility, seem to produce a reasonable number of Drell-Yan events, such that an average 5% azimuthal asymmetry is observed using realistic cut-offs and a sample of almost half million of events.

6 Acknowledgements

I thank A. Bianconi for making available his calculations of the Monte-Carlo simulations reported in sec. 5.

References

1. A. Bravar [SMC], Nucl. Phys. Proc. Suppl. **79**, 520 (1999).
2. H. Avakian [HERMES], Nucl. Phys. Proc. Suppl. **79**, 523 (1999);
A. Airapetian *et al.* [HERMES], Phys. Rev. Lett. **84**, 4047 (2000); Phys.
Rev. D**64**, 097101 (2001); Phys. Lett. B **562**, 182 (2003).
3. G. Bunce *et al.*, Phys. Rev. Lett. **36**, 1113 (1976).
4. G.L. Kane, J. Pumplin, and W. Repko, Phys. Rev. Lett. **41**, 1689 (1978).
5. J. Ralston and D.E. Soper, Nucl. Phys. B **152**, 109 (1979).
6. R.L. Jaffe, "Spin, Twist and Hadron Structure in Deep-Inelastic Processes"
in: International School of Nucleon Structure - The Spin Structure of the
Nucleon (Erice, 3-10 August 1995), hep-ph/9602236.

7. V. Barone and P.G. Ratcliffe, "Transverse Spin Physics" (World Scientific, 2003, Singapore).
8. J.C. Collins, Nucl. Phys. B **396**, 161 (1993).
9. R.L. Jaffe, X. Jin, and J. Tang, Phys. Rev. Lett. **80**, 1166 (1998).
10. A. Bianconi, S. Boffi, R. Jakob, and M. Radici, Phys. Rev. D **62**, 034008 (2000).
11. C. Caso *et al.* [Particle Data Group], Eur. Phys. J. C **3**, 1 (1998).
12. J. Soffer, Phys. Rev. Lett. **74**, 1292 (1995).
13. C. Bourrely, J. Soffer, and O.V. Teryaev, Phys. Lett. B **420**, 375 (1998).
14. W. Vogelsang, Phys. Rev. D **57**, 1886 (1998).
15. R.L. Jaffe and X. Ji, Phys. Rev. Lett. **71**, 2547 (1993).
16. A. Bravar *et al.*, Phys. Rev. Lett. **78**, 4003 (1978).
17. M. Anselmino, D. Boer, U. D'Alesio, and F. Murgia, Phys. Rev. D **63**, 054029 (2001).
18. P.J. Mulders and R.D. Tangermann, Nucl. Phys. B **461**, 197 (1996).
19. K.A. Oganessyan, N. Bianchi, E. De Sanctis, and W.-D. Nowak, Nucl. Phys. A **689**, 784 (2001).
20. D. Boer and P.J. Mulders, Phys. Rev. D **57**, 5780 (1998).
21. D. Boer, Nucl. Phys. B **603**, 195 (2001).
22. A.V. Efremov, O.G. Smirnova, and L.G. Tkatchev, Nucl. Phys. Proc. Suppl. **74**, 49 (1999); *ibidem* **79**, 554 (1999).
23. D. Sivers, Phys. Rev. D **41**, 83 (1990); *ibidem* **43**, 261 (1991).
24. D. Boer, Phys. Rev. D **60**, 014012 (1999).
25. J. Qiu and G. Stermann, Phys. Rev. Lett. **67**, 2264 (1991); Nucl. Phys. B **378**, 52 (1992).

26. S.J. Brodsky, D.S. Hwang, and I. Schmidt, Phys. Lett. B **530**, 99 (2002).
27. J.C. Collins, Phys. Lett. B **536**, 43 (2002).
28. X. Ji and F. Yuan, Phys. Lett. B **543**, 66 (2002).
29. D. Boer, P.J. Mulders, and F. Pijlman, Nucl. Phys. B **667**, 201 (2003).
30. J.C. Collins and G.A. Ladinski, hep-ph/9411444.
31. A. Bacchetta and M. Radici, Phys. Rev. D **69**, 074026 (2004).
32. M. Radici, R. Jakob, and A. Bianconi, Phys. Rev. D **65**, 074031 (2002).
33. D. Boer, R. Jakob, and M. Radici, Phys. Rev. D **67**, 094003 (2003).
34. A. Bacchetta and M. Radici, in preparation.
35. A. Bacchetta and M. Radici, Phys. Rev. D **67**, 094002 (2003).
36. A. Bacchetta and P.J. Mulders, Phys. Rev. D **62**, 114004 (2000).
37. A.V. Efremov, L. Mankiewicz, and N.A. Tornqvist, Phys. Lett. B **284**, 394 (1992).
38. A.V. Efremov and D. Kharzeev, Phys. Lett. B **366**, 311 (1996).
39. O. Martin, A. Schäfer, M. Stratmann, and W. Vogelsang, Phys. Rev. D **57**, 3084 (1998).
40. V. Barone, T. Calarco, and A. Drago, Phys. Rev. D **56**, 527 (1997).
41. A.V. Efremov, K. Goeke, and P. Schweitzer, Eur. Phys. J. **C35**, 207 (2004).
42. M. Anselmino, V. Barone, A. Drago, and N.N. Nikolaev, hep-ph/0403114, to appear in Phys. Lett. B.
43. A. Metz, Phys. Lett. B **549**, 139 (2002).
44. S. Falciano *et al.* [NA10], Z. Phys. C **31**, 513 (1986); M. Guanziroli *et al.* [NA10], Z. Phys. C **37**, 545 (1988).

45. A. Brandenburg, O. Nachtmann, and E. Mirkes, *Z. Phys. C* **60**, 697 (1993);
A. Brandenburg, S.J. Brodsky, V.V. Khoze, and D. Müller, *Phys. Rev. Lett.*
73, 939 (1994); K.J. Eskola, P. Hoyer, M. Vätinnen, and R. Vogt, *Phys.*
Lett. B **333**, 526 (1994).
46. A. Bianconi, private communication.
47. J.S. Conway *et al.*, *Phys. Rev. D* **39**, 92 (1989).